

Polysulfide Anions. 1. Structure and Vibrational Spectra of the S_2^{2-} and S_3^{2-} Anions. Influence of the Cations on Bond Length and Angle

Omar El Jaroudi,[†] Eric Picquenard,[‡] Antoine Demortier,[§] Jean-Pierre Lelieur,[§] and Jacques Corset^{*,‡}

LADIR, CNRS, 2 Rue Henri Dunant, 94320 Thiais, France, Département de Physique, Université Chouaib Doukkali, BP 20, El Jadida, Morocco, and LASIR, CNRS-HEI, 13 Rue de Toul, 59000 Lille, France

Received September 15, 1998

In a comprehensive study of the M_2S_n and $M'S_n$ alkali (M) and alkaline-earth (M') polysulfides, the alkali polysulfides K_2S_2 , $Na_2S_3 \cdot NH_3$, and K_2S_3 have been prepared by reaction of the metal with sulfur in liquid ammonia and subsequent heat treatments. Their Raman spectra have been analyzed in relation to their known X-ray structures, and that of BaS_3 has been revisited. The structure of K_2S_2 seems intermediate in the M_2S_2 , $M'S_2$ series since it has two slightly different anions in the unit cell. As for Na_2S_2 , K_2S_2 has two α and β phases but with a much higher transition temperature ~ 310 °C. These results, and those of the literature, allow the S_2^{2-} bond length to be related to the variation of its electronic structure with the cation electric field. The results obtained for the M_2S_3 and $M'S_3$ polysulfides, and those of the literature, show the existence of a low- and a high-temperature phase for K_2S_3 as for the other M_2S_3 compounds. The S_3^{2-} anion geometry, as for S_2^{2-} , is directly related to the cation electric field. The opening of the SSS angle in BaS_3 is linked to the absence of cations at short distance of both terminal sulfur atoms of the S_3^{2-} anion. It is thus shown that the bond length decreases with the polarizing power of the cations. The force field calculated for these anions are related to the SS bond length. The phase transformations and the stability of these compounds is explained by the polarizing power of the cation, which drives the volume left free for the anion in the crystal.

Introduction

The structure and reactivity of S_n^{2-} anions in solid metal polysulfides are known to be strongly related to the nature of the metallic cation. As an illustration of this influence, the phase diagrams of alkali–sulfur systems,¹ which have been thoroughly studied,^{2–7} show the existence of various M_2S_n compounds. The usual preparation method for alkali polysulfides is the thermal reaction between elemental sulfur and the alkali metal.² With this procedure, it seems that only Li_2S and Li_2S_2 can be obtained. For sodium, Na_2S_n with $n = 1, 2, 4,$ and 5 are known; Na_2S_3 is unstable and disproportionates at about 100 °C into the 1:1 eutectic Na_2S_2 – Na_2S_4 .^{6,8} For potassium, rubidium, and cesium, the M_2S_n polysulfides with $n = 1–6$ have been identified.⁷ The absence of high n values for Li polysulfides, as well as the

maximum value ($n = 5$) for Na polysulfides, is probably due to the size and to the charge of the cations as suggested by Oei.⁷

These polysulfides are usually very hygroscopic, and the Raman spectroscopy which allows their study in sealed sample tubes, is a very good tool to follow their thermal behavior. A large number of studies of the vibrational spectra of Na,^{8,9} K,^{9,10} Rb,^{11,12} Cs,^{11,12} Ba,¹³ and Sr¹⁴ polysulfides have been published, with the aim of characterizing the S_n^{2-} anion from their spectra. Very few studies^{15–17} have attempted to relate the vibrational spectra and the X-ray structure. However these structures are known for numerous polysulfides.^{1,2} To get a better insight into the structure of the various S_n^{2-} anions, our main objective was to relate the Raman spectra of the M_2S_n and $M'S_n$ polysulfides to their known X-ray structures through a force field analysis. In the present paper, we consider the M_2S_n and $M'S_n$ polysulfides with $n = 2$ and 3 . As a complement to the literature data, we have examined the Raman spectra of $Na_2S_3 \cdot NH_3$, K_2S_2 , and K_2S_3 prepared from the reaction in liquid ammonia solution

[†] Université Chouaib Doukkali

[‡] LADIR.

[§] LASIR.

- (1) Recent reviews on the sulfur–alkali metal phase diagrams. Na–S: Sangster, J.; Pelton, A. D. *J. Phase Equilib.* **1997**, *18* (1), 89. K–S: Sangster, J.; Pelton, A. D. *J. Phase Equilib.* **1997**, *18* (1), 82. Rb–S: Sangster, J.; Pelton, A. D. *J. Phase Equilib.* **1997**, *18* (1), 97. Cs–S: Sangster, J.; Pelton, A. D. *J. Phase Equilib.* **1997**, *18* (1), 78.
- (2) Cleaver, B. Properties of Polysulfide melts. In *The sulfur electrode*; Tischer, R. P., Ed.; Academic Press Inc.: 1983; Chapter II, p 35.
- (3) Sharma, R. A. *J. Electrochem. Soc.* **1972**, *119*, 1439.
- (4) Cunningham, P. T.; Johnson, E. J.; Cairns, S. A. *J. Electrochem. Soc.* **1972**, *119*, 1448.
- (5) Letoffe, J. M.; Blanchard, J. M.; Bousquet, J. *Bull. Soc. Chim. Fr.* **1976**, *3–4*, 395.
- (6) Oei, D. *J. Inorg. Chem.* **1973**, *12*, 435.
- (7) Oei, D. *J. Inorg. Chem.* **1973**, *12*, 438.
- (8) Janz, G. J.; Downey, J. R., Jr.; Roduner, E.; Wasilezyk, G. J.; Coutts, J. W.; Eluard, A. *Inorg. Chem.* **1976**, *15*, 1759.

- (9) Eysel, H. H.; Wiegardt, G.; Kleinschmager, H.; Weddigen, G. Z. *Naturforsch.* **1976**, *31b*, 415.
- (10) Janz, G. J.; Coutts, J. W.; Downey, J. R., Jr.; Roduner, E. *Inorg. Chem.* **1976**, *15*, 1755.
- (11) Bues, W.; Ziemann, H. Z. *Anorg. Allg. Chem.* **1979**, *456*, 54.
- (12) Bues, W.; Ziemann, H. Z. *Anorg. Allg. Chem.* **1979**, *455*, 69.
- (13) Janz, G. J.; Roduner, E.; Coutts, J. W.; Downey, J. R., Jr. *Inorg. Chem.* **1976**, *15*, 1751.
- (14) Chivers, T. Polychalcogenide Anions. In *New Uses of Sulfur*; West, J. R., Ed.; Advances in Chemistry 140; American Chemical Society: Washington, DC, 1975; Chapter 22, p 508.
- (15) Daly, F. P.; Brown, W. C. *J. Phys. Chem.* **1975**, *79*, 350.
- (16) Stuedel, R. *J. Phys. Chem.* **1976**, *80*, 1516.
- (17) Stuedel, R.; Schuster, F. Z. *Naturforsch.* **1977**, *32a*, 1313.

between the metal and sulfur. We have also reexamined the Raman spectrum of BaS_3 prepared from the reaction of BaS with a stoichiometric amount of sulfur at 550°C . The same type of analysis for $n = 4-6$ will be given in a forthcoming paper.¹⁸

Experimental Section

Sodium and potassium (all Fluka, >99%) were cut and weighed in a glovebox under a water-, nitrogen-, and oxygen-free argon atmosphere. The weight of sulfur (Fluka, >99.999%) was then adjusted in order to have the stoichiometry corresponding to the alkali polysulfide under preparation. Alkali metals and sulfur were weighed with an accuracy of ± 0.1 mg in order to synthesize about 5 g of a polysulfide compound. The Pyrex cell containing the alkali metal and sulfur was then transferred onto a vacuum line and pumped down to about 10^{-6} Torr, for several hours. Ammonia, dried over potassium, was then distilled and condensed on the alkali metal and sulfur at the temperature of liquid nitrogen. The amount of ammonia was not accurately controlled. It was of the order of 50–100 mL. The cell was closed with a stopcock and was then slowly warmed to 0°C . The alkali metal was solubilized much faster than sulfur in ammonia, and a blue solution of alkali metal in ammonia was then obtained. When the solution was progressively warmed, the alkali–ammonia solution reduced the sulfur and the blue color disappeared. The solution was kept for 3–4 days at 0°C in order to reach the completion of the reaction. The solution was then cooled at ca. -30°C , and ammonia was then evaporated slowly. The solution was progressively warmed while the ammonia was evaporating. When most of the ammonia had evaporated, the cell was transferred onto a vacuum line and pumped down while being heated at a given temperature. For the preparation of $\text{Na}_2\text{S}_3\cdot\text{NH}_3$, the cell was heated at ca. 60°C ; for K_2S_3 , it was heated under various conditions given in Experimental Results. The pressure reached at the end of this step depended on the heating temperature. The cell was then transferred in the glovebox and opened under an argon atmosphere. The alkali polysulfide was ground and introduced in a suprasil quartz tube of 3 mm external diameter. This tube was transferred onto a vacuum line and sealed under vacuum.

The BaS_3 compound was prepared according to the method used by Schnering and Goh.²³ Barium sulfide BaS (Alfa, >98%) and sulfur were weighed in the glovebox, in the stoichiometry required for the trisulfide, and finely ground together. This mixture was introduced in a quartz cell, which was sealed under vacuum and then heated at 550°C for 2 days. The cell was then opened in the glovebox and the BaS_3 compound ground and introduced in a suprasil tube, which was sealed under vacuum.

An XY multichannel Dilor instrument equipped with a double monochromator as filter and with a liquid nitrogen cooled Wright CCD mosaic detector (1200×300) was used to record the Raman spectra of polysulfide anions at room temperature. At liquid nitrogen temperature, the Raman spectra were recorded on a triple monochromator RTI 30 Dilor spectrometer with a spectral resolution better than 2 cm^{-1} below 1300 cm^{-1} . An Olympus microscope was coupled with the XY spectrometer, and a long front objective of magnification ($\times 80$) was used to observe the different phases formed in the sealed sample tube. Under these conditions the laser power was kept below 1 mW.

The Raman spectra were excited by 457.9, 488.0, or 514.5 nm radiation from a Spectra Physics argon ion laser.

Experimental Results

Sodium Polysulfide: $\text{Na}_2\text{S}_3\cdot\text{NH}_3$. The Raman spectrum of the compound $\text{Na}_2\text{S}_3\cdot\text{NH}_3$ prepared by reacting Na metal with

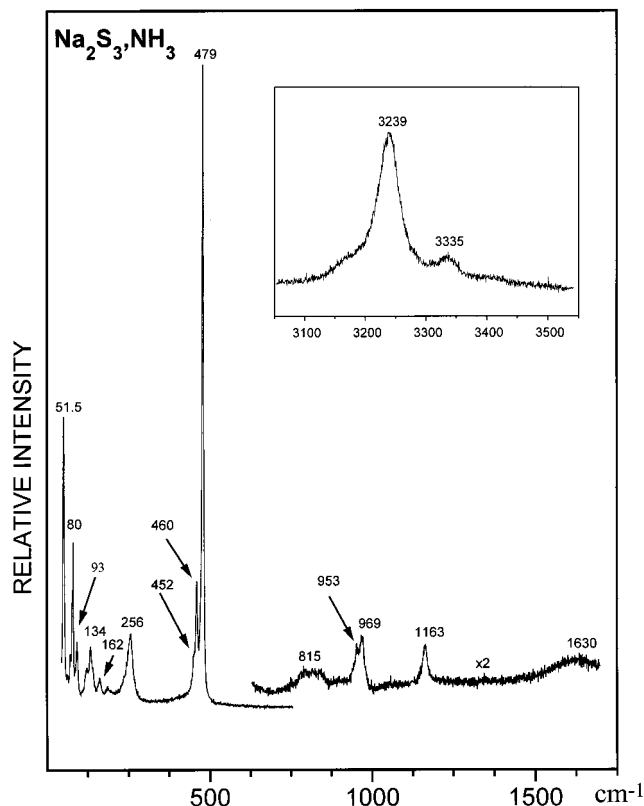


Figure 1. Raman spectrum of the compound $\text{Na}_2\text{S}_3\cdot\text{NH}_3$. XY DILOR microspectrometer: $\lambda = 514.5$ nm, integration time 300 s; between 30 and 750 cm^{-1} , $P = 0.3$ mW, slit width $140\ \mu\text{m}$, spectral slit 4.3 cm^{-1} ; between 640 and 1700 cm^{-1} , $P = 1.1$ mW, slit width $200\ \mu\text{m}$, spectral slit 6.2 cm^{-1} ; between 3050 and 3550 cm^{-1} , $P = 1.2$ mW, slit width $300\ \mu\text{m}$, spectral slit 9.3 cm^{-1} .

S_8 in liquid ammonia shows that an almost pure compound is formed (Figure 1). Only a small component (shoulder at 452 cm^{-1}) due to S_2^{2-} is observed with an intensity varying along the sample region examined with the Raman microscope. The $\nu_s(\text{SS})$ and $\nu_a(\text{SS})$ stretching vibrations are observed at 479 and 460 cm^{-1} , respectively, in good agreement with those observed by Janz *et al.*⁸ for a probably hydrated sample. The spectrum published by Janz *et al.*⁸ is indeed that of a compound prepared through a double displacement reaction from BaS_3 . This procedure leads to a mixture of Na_2S_3 and Na_2S_4 , and it seems that in water solution the S_3^{2-} anion disproportionates to S_2^{2-} and S_4^{2-} as observed when heating Na_2S_3 above 130°C .⁶ The bending $\nu_2(\text{SS})$ vibration is observed at 256 cm^{-1} in contrast with the assignment of this mode at the band observed at 238 cm^{-1} by Janz *et al.*⁸ which may be due to $\alpha\text{-Na}_2\text{S}_4$ or BaS_3 . Bands observed at wavenumbers lower than 186 cm^{-1} are due to lattice vibrations. The solvating ammonia molecule is characterized by its stretching vibrations ν_3 and ν_1 at 3335 and 3239 cm^{-1} and its bending vibrations ν_4 and ν_2 at 1630 and 1163 cm^{-1} , respectively. The band observed at 953 cm^{-1} is due to the harmonic of the $\nu_s(\text{SS})$ mode, and the components at 815 and 969 cm^{-1} probably are due to rocking modes of the ammonia molecule.¹⁹ The band wavenumbers of the ammonia molecule are very close to those observed for the solvate $\text{NaBr}\cdot 5^{1/7}\text{NH}_3$.¹⁹ This seems to indicate that the ammonia molecule, in agreement with the Na–N distances 2.56 and $2.70\ \text{\AA}$ found in the structure,²⁰ is bonded by its nitrogen lone pair to the Na^+ ions and forms hydrogen bonds with the S_3^{2-} anions such as with the Br^- anion in the $\text{NaBr}\cdot 5^{1/7}\text{NH}_3$ ammoniate.

(18) El Jaroudi, O.; Picquenard, E.; Lelieur, J. P.; Demortier, A.; Corset, J. To be published.

(19) Régis, A.; Limouzi, J.; Corset, J. *J. Chim. Phys.* **1972**, *69*, 689.

(20) Böttcher, P. *Z. Anorg. Allg. Chem.* **1980**, *467*, 149.

(21) Steudel, R. *Angew. Chem., Int. Ed. Engl.* **1975**, *14*, 655.

(22) J. Föppel, H.; Busman, E.; Foroth, F. K. *Z. Anorg. Allg. Chem.* **1962**, *314*, 13.

(23) Schnering, H. G. V.; Goh, N. K. *Naturwissenschaften* **1974**, *61*, 272.

Table 1. Structure and $\nu(\text{SS})$ Wavenumbers of the S_2^{2-} Ions in the M_2S_2 and $\text{M}'\text{S}_2$ Polysulfides. SS Bond Lengths (d_{SS}) from X-ray Data and from Vibrational Wavenumbers, Volume Left Free ($V_{\text{S}_2^{2-}}$) for S_2^{2-} Anions, Sum of Crystal Ionic Radii of M^{n+} Cation and S^{2-} Anion, and Cation Polarizing Power

	Cs_2S_2	Rb_2S_2	$\alpha\text{-K}_2\text{S}_2$	$\beta\text{-K}_2\text{S}_2$	$\alpha\text{-Na}_2\text{S}_2$	$\beta\text{-Na}_2\text{S}_2$	BaS_2	SrS_2
cryst syst	orthorhombic		hexagonal		hexagonal	hexagonal	monoclinic	tetragonal
ref	26		22		22	22	23	23
space group	$Immm$		$P62m$		$P62m$	$P6_3mmc$	$C2/c$	$I4/mcm$
Z	D_{2h}^{25}		D_{3h}^3		D_{3h}^3	D_{6h}^4	C_{2h}^6	D_{4h}^{18}
d_{SS} (X-ray), Å	2.107		2.10		2.15	2.15	2.126	2.083
spectra	11	11	a	a	24	8	25	
$\nu(\text{SS})$, cm^{-1}	472	473	469	476			473	
d_{SS} calc., ^b Å	2.123	2.122	2.126	2.119	454	451	2.122	
$V_{\text{S}_2^{2-}}$ calc., Å ³	136.5		101.8	2.140	82.9	81.8	79.3	65.2
$r_{\text{M}^{n+}} + r_{\text{S}^{2-}}$, ^c Å	3.52	3.32	3.18	2.140	2.82		3.19	2.97
polarizing power, $ne/(r_{\text{M}^{n+}})^2$, 10^3 C cm^{-2}	0.57	0.74	0.90		1.72		1.80	2.58

^a This work. ^b From the Steudel relation:²¹ $\log(f_i/\text{mdyn } \text{Å}^{-1}) = 2.66 - 7.26 \log(d_{\text{SS}}/\text{Å})$. ^c Reference 39.

Potassium Polysulfides: K_2S_2 , K_2S_3 . To check the relation between bond length and wavenumbers, for the S_2^{2-} ion,²¹ we have tried to prepare K_2S_2 . A bond length of 2.10 Å ²² is expected intermediate between those measured for Na_2S_2 ²² and BaS_2 ²³ (Table 1) and close to that found for Cs_2S_2 .²⁶ According to the potassium–sulfur phase diagram,^{1b} as shown by DSC measurements,²⁷ two forms α and β exist for K_2S_2 with a phase change temperature of 146 °C . A similar transition exists for Na_2S_2 at 170 °C .^{1a} The structure determined by Föppl *et al.* for K_2S_2 ²² is that of a product prepared from potassium metal and sulfur in liquid ammonia as previously done by Feher *et al.*²⁸ This product had a density of 1.79 g/cm^3 , after heating at 60 °C during 4 days. It was further heated at 320 °C under a nitrogen atmosphere. The product obtained after this treatment had a density of 1.89 g/cm^3 . The authors pointed out that the two products, before and after heating at 330 °C , showed the same X-ray diagram. Nevertheless, they reported that some lines which appeared diffuse before heating became sharp. This compound had a hexagonal structure with the space group $P62m$, D_{3h}^3 , and is isomorphous of the $\alpha\text{-Na}_2\text{S}_2$ phase. The unit cell contains three formula units ($Z = 3$), two sulfur atoms S(1) forming an $\text{S}(1)\text{S}(1)^{2-}$ anion are located in sites (e) with $z_1 = 0.320$ and four sulfur atoms S(2) forming two $\text{S}(2)\text{S}(2)^{2-}$ anions are located in sites (h), with $z_2 = 0.180$. The relation $z_1 = 1/2 - z_2$ proposed by the authors implies that the three S_2^{2-} anions have the same bond length.

The spectrum of the product we have prepared from liquid ammonia and heated to 80 °C under high vacuum is shown in Figures 2 and 3a. This spectrum contains four main lines at 454.5 , 462 , 469 , and 476 cm^{-1} in the $\nu(\text{SS})$ stretching vibration region and three lattice vibrations at 87 , 118 , and 148 cm^{-1} . This spectrum changed only slowly when the product was heated to 210 °C during several hours (Figure 3b). When the product was heated above 320 °C , the two central lines disappeared more rapidly (Figure 3c). Finally the spectrum of the compound heated to 320 °C for 30 h under a 0.5 atm pressure of NH_3 was recorded (Figure 3c and Figure 4). This spectrum, recorded at room temperature, has two main lines at 454 and 476 cm^{-1} , with

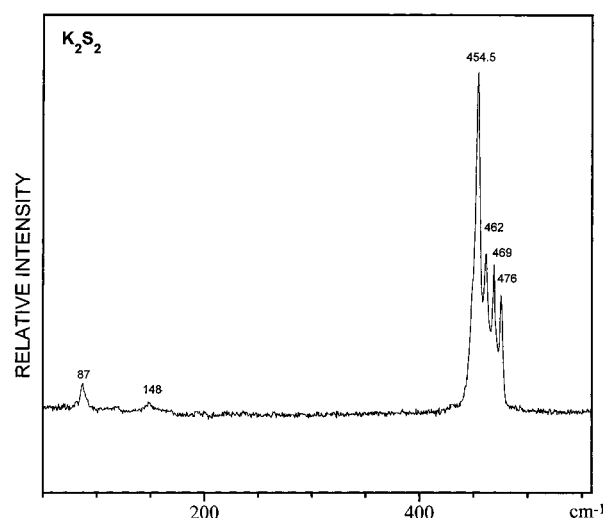


Figure 2. Raman spectrum of the compound of stoichiometry K_2S_2 , (a) dried at 80 °C . XY DILOR microspectrometer: $\lambda = 514.5 \text{ nm}$, $P = 3.2 \text{ mW}$, integration time 900 s, slit width $80 \mu\text{m}$, spectral slit 2.5 cm^{-1} .

shoulders on the low wavenumber side of these two components. These shoulders have first been assumed to be due to isotopic components belonging to the species $(^{32}\text{S}^{34}\text{S})^{2-}$ since its abundance is 8% compared to the 90% abundance of the $(^{32}\text{S}^{32}\text{S})^{2-}$ species. The poor agreement of the summation spectrum with the observed one (Figure 4a) implies the existence of a hot band, distant from the main band by twice the anharmonicity constant $\omega_e x_e = 2.1 \text{ cm}^{-1}$, deduced from the observation of the $2\nu(\text{SS})$ harmonic of the main band. This value has a good order of magnitude compared to the $\omega_e x_e$ values of 2.852 and 2.5 cm^{-1} measured for S_2 and S_2^{2-} , respectively.²⁹ The good agreement of the summation spectrum with the observed one (Figure 4b), and the spectrum observed at liquid nitrogen temperature (Figure 4c), confirm the assignment of the intermediate component to the transition $\nu_i = 1 \rightarrow \nu_i = 2$. Indeed this hot band is not observed in the liquid nitrogen temperature spectrum which allows observation of the isotopic $(^{34}\text{S}^{32}\text{S})^{2-}$ components in the expected intensity ratio with the $(^{32}\text{S}^{32}\text{S})^{2-}$ components. We can conclude that the spectrum of the phase obtained by heating above 320 °C corresponds to a crystal

(24) Eysel, H. H.; Wieghardt, G.; Kleinschmager, H.; Weddigen, G. Z. *Naturforsch.* **1976**, *B21*, 415.

(25) Steudel, R. Z. *Naturforsch.* **1975**, *30b*, 281.

(26) Böttcher, P. J. *Less Common Met.* **1979**, *63*, 99.

(27) Janz, G. J.; Rogers, D. J. J. *Chem. Eng. Data* **1983**, *28* (3), 331.

(28) Feher, F.; Berthold, H. J. Z. *Anorg. Allg. Chem.* **1953**, *274*, 223.

(29) Clark, R. J. H.; Cobbold, D. J. *Inorg. Chem.* **1978**, *17*, 3169.

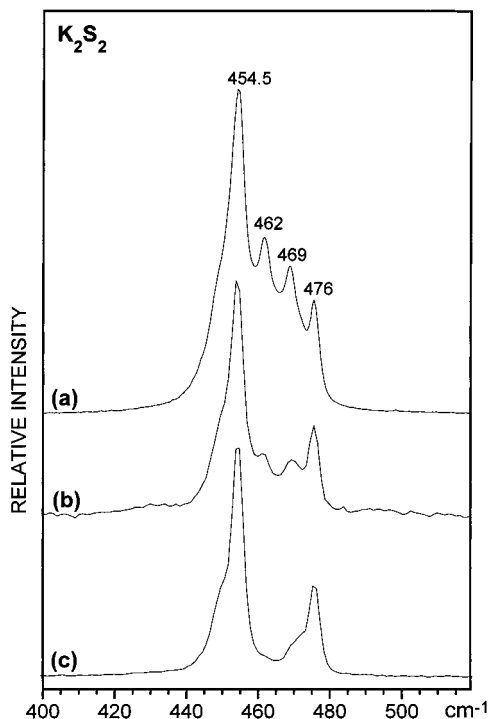


Figure 3. Raman spectrum of the compound of stoichiometry K_2S_2 , after heating at different temperatures: (a) dried at 80 °C; (b), heated at 200 °C for 86 h; (c), heated at 330 °C for 20 h. XY DILOR: spectrometer $\lambda = 514.5$ nm, $P = 3.2$ mW, slit width 80 μm , spectral slit 2.5 cm^{-1} , integration time 900 s; (b) $\lambda = 488.0$ nm, $P = 0.3$ mW, slit width 120 μm , spectral slit 4.2 cm^{-1} , integration time 600 s; (c) $\lambda = 488.0$ nm, $P = 3.3$ mW, slit width 100 μm , spectral slit 3.5 cm^{-1} , integration time 180 s.

having two types of S_2^{2-} anions in the unit cell. The small wavenumber shift between the two $\nu(\text{SS})$ vibrations at 476 and 454 cm^{-1} with an intensity ratio of *ca.* $1/2$ suggests that the crystal structure corresponds to the hexagonal D_{3h}^3 one proposed by Föppl *et al.*²² In fact, these authors have determined the unit cell parameters with an accuracy of 0.01 Å. This low accuracy did not allow them to distinguish a slight bond length difference of the S_2^{2-} ions, formed respectively by atoms in sites (e) and (h). The SS bond length estimated using the Steudel relation²¹ is 2.120 Å for S(1)S(1) $^{2-}$ and 2.140 Å for S(2)S(2) $^{2-}$. The z_1 and z_2 coordinates of the S(1) and S(2) atoms should be 0.318 and 0.183, respectively, compared to 0.320 and 0.180 for the three equivalent bond lengths assumed by Föppl *et al.*²²

The two components at 462 and 469 cm^{-1} which disappeared by heating of the compound above 310 °C (Figure 3) are due to an α phase of K_2S_2 with a structure very close to the preceding one.²² In this hexagonal structure the S_2^{2-} types of anions are still slightly different with SS bond lengths of 2.123 and 2.126 Å according to the Steudel relation.²¹

Two samples of K_2S_2 which have been heated at 320 °C for 30 h and at 330 °C for 20 h show some small crystals with spectra different from those of the K_2S_2 high-temperature β phase. These spectra have been distinguished from those of K_2S_2 with a Raman microscope and are shown in Figure 5. The first one (Figure 5a) shows one stretching vibration band at 466 cm^{-1} and a bending vibration band at 238 cm^{-1} , and it is the K_2S_3 spectrum already observed by Janz *et al.*¹⁰ The second one (Figure 5b) has two stretching vibration bands at 441 and 476 cm^{-1} and one bending vibration at 219 cm^{-1} , like the high-temperature phase of Cs_2S_3 and Rb_2S_3 (Table 3). It also contains the low-temperature phase of K_2S_3 as traces. We thus think that

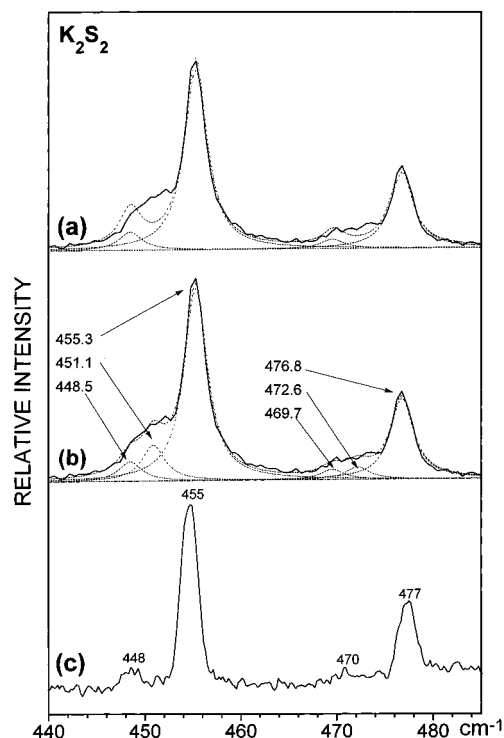


Figure 4. Raman spectrum of the K_2S_2 compound (a, b) at room temperature and (c) at liquid nitrogen temperature. Comparison with the summation spectrum of a two- or three-component analysis, assuming (a) isotopic components or (b) isotopic components and hot bands. (a, b) XY DILOR spectrometer: $\lambda = 488.0$ nm, $P = 0.3$ mW, slit width 50 μm , spectral slit 1.8 cm^{-1} , integration time 1800 s. (c) Spectrometer triple monochromator RTI DILOR: $\lambda = 514.5$ nm, $P = 60$ mW, slit width 200 μm , spectral slit 1.4 cm^{-1} .

these spectra can be due to the formation of K_2S_3 through the disproportionation of K_2S_2 along the reaction



where M is K, Rb, or Cs. The polysulfide Cs_2S_2 has indeed been shown to undergo such a disproportionation at 100 °C.¹¹ The bands observed at 441 and 476 cm^{-1} are assigned respectively to the $\nu_s(\text{SS})$ and $\nu_a(\text{SS})$ vibration modes of the S_3^{2-} anion. The harmonics are observed at 874 and 954 cm^{-1} , and the band observed at 130 cm^{-1} is due to a lattice mode.

Barium Polysulfide: BaS_3 . The Raman spectrum of the BaS_3 sample prepared from the reaction of BaS with a stoichiometric amount of S_8 (Figure 6) shows only the two stretching vibrations at 479 and 458 cm^{-1} . They are assigned to the $\nu_a(\text{SS})$ and $\nu_s(\text{SS})$ vibrations, respectively, in good agreement with the observation by Janz *et al.*¹³ at 476 and 458 cm^{-1} , with a shoulder at 412 cm^{-1} and a band at 402 cm^{-1} , the last two components being not observed here (Figure 6 and Table 3). The $\delta(\text{SSS})$ bending mode observed at 229 cm^{-1} is superimposed on a broader component at *ca.* 239 cm^{-1} assigned to a combination of lattice modes ($156 + 85 = 241$ cm^{-1}). The harmonics $2\nu_a(\text{SS})$ and $2\nu_s(\text{SS})$ at 955 and 917 cm^{-1} and the combinations $\nu_s + \delta$ and $\nu_a + \delta$ at 690 and 710 cm^{-1} are observed as single bands. This confirms the existence of only one type of S_3^{2-} anion in this compound.

Discussion

Bond Length Dependence of the S_2^{2-} Anion on the Cation Electric Field. We have summarized in Table 1 the $\nu(\text{SS})$ wavenumbers and the structures known for the M_2S_2 and $M'S_2$

Table 2. Short MS Distances (Å) and MSM Angles (deg) in the Cationic Environment of the S_2^{2-} Anion in the Cs_2S_2 , Na_2S_2 , BaS_2 , and SrS_2 Crystal Unit Cells

$Cs_2S_2^{26}$	$Na_2S_2^{22}$	BaS_2^{23}	SrS_2^{23}
Distances			
Cs(1)S = Cs(3)S = 3.645	Na(1)S = 2.827	Ba(1)S(1) = Ba(6)S(2) = 3.167	Sr(1)S = Sr(2)S = 3.088
Cs(1')S = Cs(3')S = 3.645	Na(2)S = 2.966	Ba(1)S(2) = Ba(6)S(1) = 3.220	
Cs(2)S = Cs(2')S = 3.518		Ba(2)S(1) = Ba(5)S(2) = 3.236	
		Ba(4)S(1) = Ba(3)S(2) = 3.241	
Angles			
Cs(1)SCs(2) = 95.8	Na(2)SNa(2) = 92.9	Ba(1)S(1)Ba(2) = 97.6	Sr(1)SSr(2) = 76.5
Cs(3)SCs(2) = 130.1	SNa(1)S = 44.6	Ba(2)S(1)Ba(4) = 121.5	Sr(2)SSr(2) = 88.6
Cs(1)SCs(3) = 75.9		Ba(4)S(1)Ba(1) = 109.8	Sr(1)SSr(1) = 88.6

Table 3. Structure and Vibrational Wavenumbers of the S_3^{2-} Anion in the M_2S_3 and $M'S_3$ Polysulfides. Volume Left Free ($V_{S_3^{2-}}$) and Valence Force Field for the S_3^{2-} Anion

	Cs_2S_3		Rb_2S_3		K_2S_3		Na_2S_3	$Na_2S_3 \cdot NH_3$	BaS_3		SrS_3
cryst syst	orthorhombic		orthorhombic		orthorhombic			monoclinic	tetragonal		orthorhombic
ref	37		37		38			20	23		23
space group	$Cmc2_1$		$Cmc2_1$		$Cmc2_1$			$C2/m$	$P42_1m$		$B2cb$
	C_{2v}^{12}		C_{2v}^{12}		C_{2v}^{12}			C_{2h}^3	D_{2d}^3		C_{2v}^{17}
Z	4		4		4			4	2		4
$d(SS)$, Å	2.122		2.102		2.083			2.078	2.074		2.050
$\alpha(SSS)$, deg	106.03		106.59		105.4			106.5	114.8		106.6
$V_{S_3^{2-}}$, Å ³	132.0		124.8		115.7			97.7 ^k	88.8		93.5
spectra	<i>a</i>	<i>b</i>	<i>a</i>	<i>b</i>	<i>c, d</i>	<i>e</i>	<i>f</i>	<i>g</i>	<i>h</i>	<i>i</i>	<i>j</i>
$\nu_a(SS)$, cm ⁻¹	467	492	465	487	466	476	476	479	476 (472)	479	491
$\nu_s(SS)$, cm ⁻¹	467	476	465	475	466	441	458	460	458	458	478
$\delta(SSS)$, cm ⁻¹	235	219	236	219	238	219	238	256	227 (238)	229	(219)
force field											
f_r , m dyn Å ⁻¹	1.940		2.078		2.219			2.259		2.290	2.493
f_{rr} , m dyn Å ⁻¹	0.135		0.295		0.413			0.517		0.527	0.506
$r_{f_{ra}}$, m dyn	0		0.191		0.440			0.439		0.449	0.662
$r^2 f_{ra}$, m dyn Å	1.540		1.369		1.345			1.518		1.139	1.198

^a Reference 11. Low-temperature phase. ^b Reference 11. Phase appearing under heating. ^c Reference 10. ^{d,e} This work low- and high-temperature phase. ^f Reference 8. ^g This work. ^h Reference 13. ⁱ This work. ^j Reference 15. ^k This volume was measured assuming for the NH_3 molecule its volume in the liquid state.

polysulfides. It can be noticed that the calculated bond lengths d_{SS} for the S_2^{2-} anions from the observed wavenumbers, using the Stuedel relation,²¹ are in relatively good agreement with the X-ray measured one. From these observations, only two types of bond lengths are found for S_2^{2-} : 2.12 Å for Cs_2S_2 , Rb_2S_2 , and BaS_2 and 2.14 Å for α - Na_2S_2 and β - Na_2S_2 . K_2S_2 seems to be an intermediate case, showing the two types of bond lengths with two nonequivalent anions in the unit cell. The various cationic environments for the S_2^{2-} anion in the crystal unit cell are shown in Figure 7, and the short MS distances found for the closest cations surrounding the S_2^{2-} anion are reported in Table 2. The SS bond length observed does not vary simply with the cation polarizing power $ne/(r_{M^{n+}})^2$ where ne is the cation charge (Table 1). Although it is difficult to describe precisely the influence of the polarizing power of the cations on the electronic distribution inside the S_2^{2-} anion, some remarks could be made on the arrangement of the neighboring cations at short distances from the sulfur atoms of the S_2^{2-} anion. Three of these structures exhibit cations that are at an almost equal distance from both sulfur atoms, bridging the S_2^{2-} anion. The MS distances of these bridging cations are the shortest and are very close to the sum of the crystal ionic radii of the cation³⁹ and of

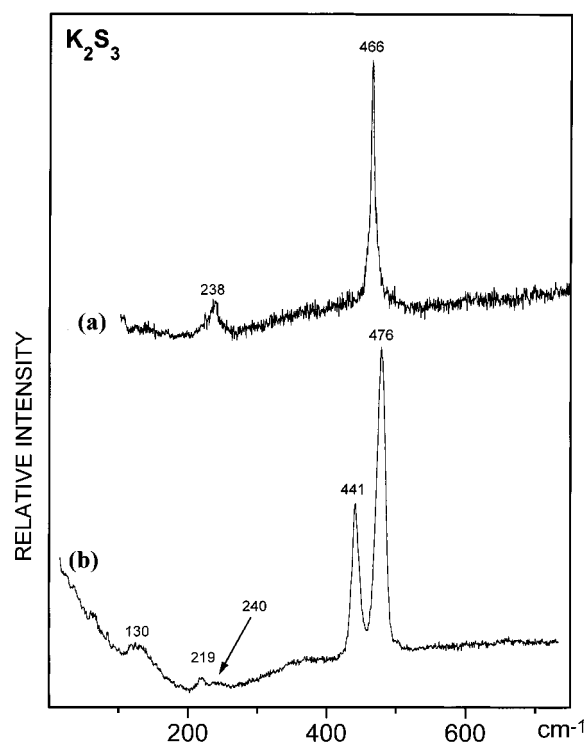


Figure 5. Raman spectrum of the two forms of K_2S_3 obtained after heating of K_2S_2 at 330 °C during 20 h. XY DILOR microspectrometer: (a) $\lambda = 514.5$ nm, $P = 0.9$ mW, slit width 80 μ m, spectral slit 2.5 cm^{-1} , integration time 600 s; (b) $\lambda = 457.9$ nm, $P = 0.25$ mW, slit width 120 μ m, spectral slit 4.8 cm^{-1} , integration time 600 s.

- (30) Herzberg, G. *Molecular Spectra and Molecular Structure, Vol. 1, Spectra of Diatomic Molecules*, 2nd ed.; D. van Nostrand Co. Inc.: Princeton, Toronto, New York, London, 1950; p 134.
- (31) Cotton, F. A.; Horman, J. B.; Hedges, R. M. *J. Am. Chem. Soc.* **1976**, *98*, 1417.
- (32) Walsh, A. D. *J. Chem. Soc.* **1953**, 2260.
- (33) Salahub, D. R.; Foti, A. E.; Smith, V. H., Jr. *J. Am. Chem. Soc.* **1978**, *100*, 7847.
- (34) Meyer, B.; Spitzer, K. *J. Phys. Chem.* **1972**, *76*, 2274.

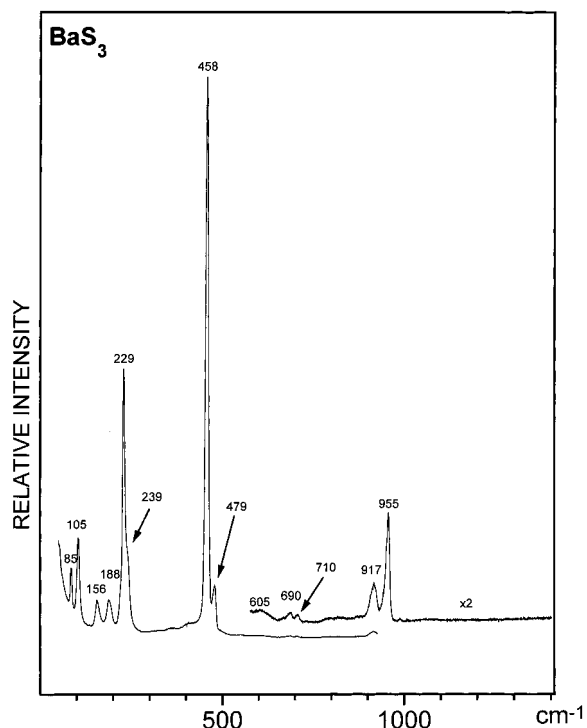


Figure 6. Raman spectrum of BaS_3 obtained by reaction of BaS and S_8 at 500°C . XY DILOR microspectrometer: $\lambda = 514.5\text{ nm}$, $P = 2.8\text{ mW}$, spectral slit 6.2 cm^{-1} , integration time 30 s between 50 and 930 cm^{-1} and 60 s between 580 and 1400 cm^{-1} .

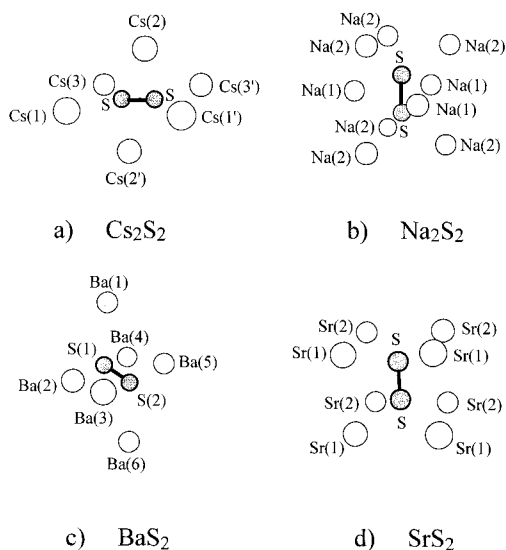


Figure 7. Neighboring cations at short distance of the S_2^{2-} anion in the unit cell of the M_2S_2 or $\text{M}'\text{S}_2$ polysulfide. For the MS distances see Table 2.

the S^{2-} anion (Tables 1 and 2). The MS distances for cations that are at a short distance from only one sulfur of the anion are longer.

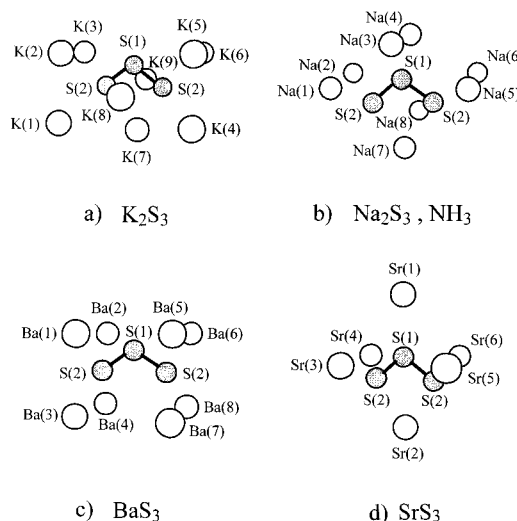


Figure 8. Neighboring cations at short distances of the S_3^{2-} anions in the unit cell of the M_2S_3 or $\text{M}'\text{S}_3$ polysulfides. For the MS distances see Table 4.

For the SrS_2 structure, where no bridging cations are observed (Figure 7), the SrS distances are longer than the sum of the ionic radii by 0.11 \AA . This is probably due to the cation–cation repulsion, while the cation polarization of the electronic charge of the anion induces a shortening of the SS bond.

The comparison of the electronic structure of the S_2 molecule having the $^3\Sigma_g^-$ electronic configuration³⁰ $\{\text{KKLL}(\sigma_g 3s)^2(\sigma_u 3s)^2(\sigma_g 3p)^2(\pi_u 3p)^4(\pi_g 3p)^2\}$ to that of the S_2^- and S_2^{2-} anions having the electronic configurations $^2\Pi_g$ and $^1\Sigma_g^+$, respectively, shows that the antibonding orbital ($\pi_g 3p$) is successively filled by one and two charge electrons. This induces a lengthening of the SS bond, as already noticed by Chivers¹⁴ and Clark,²⁹ and is confirmed by a SCF X- α calculation by Cotton *et al.*³¹ for the S_2^- anion. Thus, the influence of the cation electric field on the electronic charges located in this ($\pi_g 3p$) antibonding orbital explains the observed bond length change observed. The strong polarizing power of the Sr^{2+} cation induces a displacement of the electronic charge toward the sulfur atoms, depleting the ($\pi_g 3p$) antibonding orbital population. This explains the short SS bond observed, 2.08 \AA . At the opposite for Na_2S_2 , the three bridging cations, which prevent the depletion of the antibonding orbital population, are responsible for the unexpected long SS bond observed, 2.15 \AA , compared to that of Cs_2S_2 , 2.10 \AA . This shows that the variation of the filling of the ($\pi_g 3p$) antibonding orbital with the cation polarizing power and the position of the cations which may bridge the SS bond or mainly interact with a sulfur atom explains the observed bond length variations.

Structure and Force Field Dependence of the S_3^{2-} Anion on the Cation Electric Field. The various cationic environments of the S_3^{2-} anions of the M_2S_3 and $\text{M}'\text{S}_3$ polysulfides are shown in Figure 8, and the short MS distances for the closest cations surrounding the S_3^{2-} anion are reported in Table 4. Four types of cations may be distinguished in these environments. The two first species are similar to those observed for S_2^{2-} : cations interacting with one terminal S(2) atom only, as K(1), K(2), K(3) or K(4), K(5), K(6) for K_2S_3 , and cations bridging the S(2)S(1) bonds as K(8) and K(9). Two other types of cations of importance for the S_3^{2-} structure may be distinguished: cations interacting at an equal short distance from both S(2) terminal atoms as K(7), Sr(2), and K(8), K(9), Na(7), Na(8) which also interacts with S(1), and cations interacting with S(1) only. The shortest MS distances close to the sum of the ionic

(35) Berghof, V.; Sommerfeld, T.; Cederbaum, L. S. *J. Phys. Chem. A* **1998**, *102*, 5100.

(36) Josien, M. L.; Sourisseau, G. In *Nouveau traité de Chimie Minérale. Tome XIII. Structure des sulfures métalliques*; Pascal, P., Masson et Cie: 1960; pp 1086, 1107.

(37) Böttcher, P. Z. *Anorg. Allg. Chem.* **1960**, *461*, 13.

(38) Böttcher, P. Z. *Anorg. Allg. Chem.* **1977**, *432*, 167.

(39) *Handbook of Chemistry and Physics*, 46th ed.; Weast, R. C., Selby, S. M., Hodgman, C. D., Eds.; The Chemical Rubber Co.: Cleveland, OH, 1965–1966; p F 117.

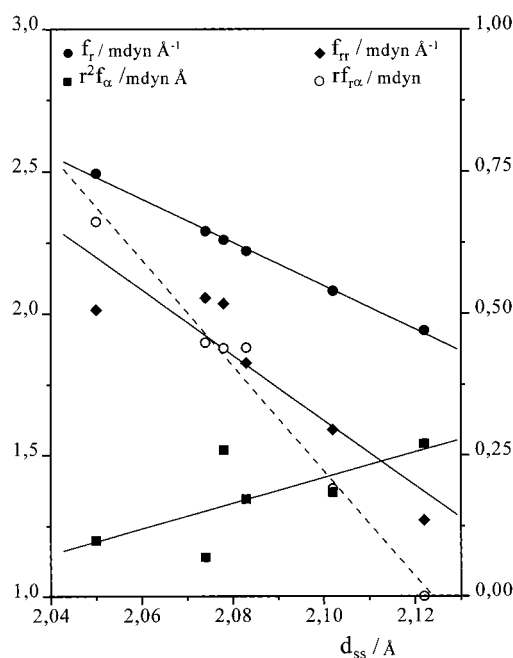
Table 4. Short MS Distances (Å) in the Cationic Environment of the S_3^{2-} Anion in the K_2S_3 , Rb_2S_3 , Cs_2S_3 , $Na_2S_3 \cdot NH_3$, BaS_3 , and SrS_3 Crystal Unit Cells

	$Cs_2S_3^{37}$	$Rb_2S_3^{37}$	$K_2S_3^{38}$	$Na_2S_3 \cdot NH_3^{20}$	BaS_3^{23}	SrS_3^{23}
M(1)S(2) = M(4)S(2)	3.604	3.423	3.292	Na(1)S(2) = Na(5)S(2) = 2.921	Ba(1)S(1) = Ba(2)S(1) = 3.205	Sr(1)S(1) = 3.304
M(2)S(2) = M(5)S(2)	3.617	3.454	3.329	Na(2)S(2) = Na(6)S(2) = 2.901	Ba(5)S(1) = Ba(6)S(1) = 3.205	Sr(2)S(2) = 3.041
M(3)S(2) = M(6)S(2)	3.448	3.306	3.178	Na(7)S(2) = 2.912	Ba(1)S(2) = Ba(2)S(2) = 3.205	Sr(3)S(2) = Sr(6)S(2) = 3.006
M(7)S(2)	3.658	3.504	3.367	Na(8)S(2) = 2.910	Ba(5)S(2) = Ba(6)S(2) = 3.205	Sr(4)S(2) = Sr(5)S(2) = 3.030
M(8)S(2)	3.657	3.502	3.347	Na(3)S(1) = 2.960	Ba(3)S(2) = Ba(4)S(2) = 3.242	
M(8)S(1)	3.534	3.389	3.247	Na(4)S(1) = 2.884	Ba(7)S(2) = Ba(8)S(2) = 3.242	
M(9)S(2)	3.509	3.350	3.231	Na(7)S(1) = 3.451		
M(9)S(1)	3.448	3.234	3.105	Na(8)S(1) = 3.286		

radii of the metal cation and the S^{2-} anion do not correspond to a particular type of interacting cations such as the bridging cations for the disulfides. Distances shorter than the ionic radii sum may even be found for M(3)S(2), M(6)S(2), and M(9)S(1) in the three isotype compounds Cs_2S_3 , Rb_2S_3 , and K_2S_3 , indicating a strong polarization of the sulfur electronic surroundings. The importance of the cations interacting with both S(2) terminal atoms may be noticed since for the three structures shown in Figure 8, namely, a, b, and d, that exhibit such cations, three, two, and one, respectively, the S(2)S(1)S(2) angle remains close to 106° . The lack of such cations in the BaS_3 structure (Figure 8c) seems thus responsible for the opening to 114.8° of the S(2)S(1)S(2) angle.

We observe that the SS bond length in the S_3^{2-} anion decreases from 2.12 to 2.05 Å as the polarizing power of the cation $ne/(r_M^{n+})^2$ increases (Tables 1 and 3). According to the Walsh diagram for the orbitals of a bent AB_2 molecule, the lowest unoccupied molecular orbital is of b_1 symmetry and is antibonding along the AB bond and slightly bonding along the BB direction.³² As it was already noticed from a molecular orbital study of the structural changes of S_3 on reduction,³³ going from the S_3 molecule to the S_3^- and S_3^{2-} anions, the $b_1(\pi)$ level of S_3 is successively occupied by one and two electrons, decreasing thus the SSS angle from 120° for S_3 and increasing the SS bond lengths according to the antibonding character of this orbital.³⁴ The bridging cations and those interacting with mainly the S(1) central atom both contribute to maintain the electronic charge in this $b_1(\pi)$ antibonding orbital. In contrast, the cations interacting with only one or symmetrically with both S(2) terminal atoms contribute to the depletion of the antibonding orbital, the electronic charge being then localized on the S(2) terminal atoms. The progressive balance of the electronic charge from the S(1)S(2) bond to the S(2) terminal atom, which increases with the polarizing power of the cations, explains the shrinkage of the SS bond.

We have summarized in Table 3 our results and those of the literature for the Raman spectra of the different M_2S_3 and $M'S_3$ polysulfides with their known crystallographic structures. Most of these polysulfides exhibit two phases, one at low temperature and the other at high temperature. The structure of the low-temperature phase was determined, but the structure of the high-temperature phase is unknown. It is indeed surprising to find very similar spectra for the low-temperature phase of the three isotype compounds Cs_2S_3 , Rb_2S_3 , and K_2S_3 , while the bond length decreases from 2.122 to 2.083 Å. To understand the spectra of these S_3^{2-} anions, we have calculated a valence force field for these anions, using their known geometry. We have assumed the C_{2v} symmetry for the S_3^{2-} anion. Four force constants were considered in this valence force field calculation: two diagonal constants f_r and r^2f_α respectively for the stretching and bending motions, and two off-diagonal ones f_{rr} and $rf_{r\alpha}$ for bond–bond and bond–angle interactions, respectively. As we have only three observed wavenumbers, the valence stretching vibrations being sometimes accidentally degenerated, as already

**Figure 9.** Force constant variations with the bond lengths of the S_3^{2-} anions in the M_2S_3 and $M'S_3$ polysulfides.

noticed by Janz *et al.*,¹⁰ we have taken for f_r the value calculated from the Steudel relation.²¹ The f_{rr} bond–bond interaction force constant is then calculated from the $\nu_a(SS)$ antisymmetric stretching vibration. The two other force constants r^2f_α and $rf_{r\alpha}$ are then calculated from the two symmetric vibrations, $\nu_s(SS)$ and $\delta(SSS)$, with the symmetric force constant $f_r + f_{rr}$ fixed. The force fields, calculated for each compound, are summarized in Table 3, and the force constants were plotted versus the SS bond length in Figure 9. In the bond length region considered, a straight line approximates well the Steudel relation for the stretching force constant. It is also seen that the points for the other force constants may be gathered around straight lines. The force field calculated for SrS_3 assumes a bending wavenumber similar to that observed for the high-temperature phase of Cs_2S_3 and Rb_2S_3 , which have close stretching wavenumbers. As we have seen before, when the polarizing power of the cation increases, the electronic charges of the S_3^{2-} anion are localized onto the S(2) terminal atoms, decreasing the bond length and increasing the f_r constant. This electronic displacement increases the bond polarity and increases, in the approximation of a dipole–dipole interaction, the f_{rr} bond–bond interaction constant. In the approximation of uncoupled symmetric stretching and bending vibrations, the equality of the $\nu_a(SS)$ and $\nu_s(SS)$ wavenumbers, called accidental degeneracy, leads to the following relation between f_r and f_{rr} for the S_3^{2-} anion: $\cos \alpha = -2f_{rr}/f_r$. This simple relation confirms that in the series Cs_2S_3 , Rb_2S_3 , K_2S_3 , for which an accidental degeneracy is observed, f_{rr} must increase with f_r since α does not vary. The α angle,

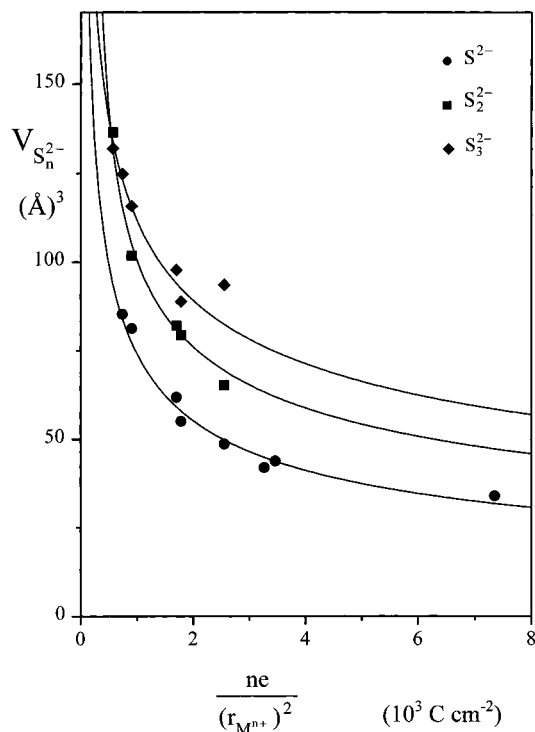


Figure 10. Volume left free for the S^{2-} , S_2^{2-} , and S_3^{2-} anions in the unit cell versus the polarizing power of the cation.

calculated from our force field with the crude approximation of uncoupled symmetric bending and stretching vibrations, is of the order of magnitude expected for an accidental degeneracy. The general increase of the bending r^2f_α force constant with the bond lengthening is mainly due to the interactions between the electron-bond. This is confirmed by the low r^2f_α value calculated for BaS_3 where the angle is much more opened: 114.8° compared to 106° .

Influence of Phase Transformations and Cations. From the known X-ray structure of the compounds, we can deduce the volume left free for the polysulfide anion in the unit cell, assuming an ionic character for these compounds. They have been summarized in Tables 1 and 2 and in Figure 10, where they are plotted versus the polarizing power of the cations $ne/(r_{M^{n+}})^2$. We have also plotted the volume left free for the sulfide anion for the known alkali and alkaline-earth sulfides which crystallize in the face centered cubic system.³⁶ Although the

metal-sulfur distances remain close to the sum of the cation ionic radius and the atomic sulfur radius, we can notice (Figure 10) that the volume available for the S^{2-} anion decreases strongly with the polarizing power of the cation, tending for Mg^{2+} toward the volume of the sulfur atom as calculated from the rhombic sulfur S_8 structure, 25.8 \AA^3 . The increase of the volume available for the S_2^{2-} anion follows also that of the sulfide S^{2-} anion from the more polarizing cations to the potassium, which we have shown to be intermediate between sodium and rubidium, since for this cation two types of anions with different bond lengths exist in the unit cell. From this point, the S_2^{2-} anion available volume increases steeply, becoming larger than that of S_3^{2-} in Cs_2S_3 . This is probably the reason why Cs_2S_2 becomes unstable under a slight heating and transforms to Cs_2S and Cs_2S_3 around 100°C as shown by Bues *et al.*¹¹ As it is known that the small sulfur dianion clusters in the gas phase are very unstable,³⁵ these results show that their instability is coming from their bond dissociation due to the filling of their ($\pi_g 3p$) antibonding orbital. Their stabilization in the solid state results, as we have shown it, from the attraction of the electron charge onto the terminal atoms under the cationic electric field.

The low-temperature phase of the alkaline trisulfides seems to behave as the sulfide anion with regard to the cation polarizing power. However, Na_2S_3 seems only to exist at low temperature and disproportionates giving the eutectic $Na_2S_2 + Na_2S_4$ as soon as heated at 130°C .⁸ The peculiar structure of BaS_3 behaves also as the low-temperature phase of the other alkaline trisulfides. The known structure of SrS_3 corresponds to an S_3^{2-} available volume higher than that expected from the other trisulfides (Figure 10). Its spectrum, reported by Chivers,¹⁴ seems to indicate a similarity to the high-temperature phase of the other trisulfides. Thus, at least two types of structures of the S_3^{2-} anion should exist for the trisulfides. One metastable structure for the alkali cations, where the electronic charges are strongly polarized by the cations and localized on the terminal atoms, has short bonds. The other structure corresponding to the low-temperature phase is also stabilized by the partial localization of the electron charge on the $S(2)$ terminal atoms. In this structure the bond length varies with the polarizing power of the cation. The SrS_3 structure could then be a stable form corresponding to the metastable high-temperature phase of the alkali trisulfides.